Computational modeling of the thermal conductivity of single-walled carbon nanotube–polymer composites

2008 Nanotechnology 19 065702

(http://iopscience.iop.org/0957-4484/19/6/065702)

Nanotechnology **19** (2008) 065702 (8pp) doi:10.1088/0957-4484/19/6/065702

Computational modeling of the thermal conductivity of single-walled carbon nanotube–polymer composites

Hai M Duong[1], **Dimitrios V Papavassiliou**[2], **Kieran J Mullen**[3] **and Shigeo Maruyama**[1]

[1] Department of Mechanical Engineering, The University of Tokyo, Japan
[2] School of Chemical, Biological and Materials Engineering, The University of Oklahoma, USA
[3] The Homer L Dodge Department of Physics and Astronomy, The University of Oklahoma, USA

E-mail: maruyama@photon.t.u-tokyo.ac.jp

Received 6 September 2007, in final form 22 November 2007
Published 23 January 2008
Online at stacks.iop.org/Nano/19/065702

Abstract

A computational model was developed to study the thermal conductivity of single-walled carbon nanotube (SWNT)–polymer composites. A random walk simulation was used to model the effect of interfacial resistance on the heat flow in different orientations of SWNTs dispersed in the polymers. The simulation is a modification of a previous model taking into account the numerically determined thermal equilibrium factor between the SWNTs and the composite matrix material. The simulation results agreed well with reported experimental data for epoxy and polymethyl methacrylate (PMMA) composites. The effects of the SWNT orientation, weight fraction and thermal boundary resistance on the effective conductivity of composites were quantified. The present model is a useful tool for the prediction of the thermal conductivity within a wide range of volume fractions of the SWNTs, so long as the SWNTs are not in contact with each other. The developed model can be applied to other polymers and solid materials, possibly even metals.

(Some figures in this article are in colour only in the electronic version)

1. Introduction

The incorporation of SWNTs into composite materials can enhance their mechanical and electrical transport properties [1]. The presence of SWNTs can also enhance the thermal transport [2, 3], allowing possible applications of SWNTs in nanotube composite layers to be used as thermal shields and thermal conductors. Since SWNTs have unique properties [4], the properties and the full potential of SWNT-based composites, which have not yet been fully investigated, are expected to be superior. Uniform dispersion and alignment of nanotubes within the polymer matrix are fundamental requirements for producing composites with reproducible and optimal properties.

Bryning *et al* [5] reported thermal conductivity measurements of purified SWNT–epoxy composites prepared using suspensions of SWNTs in *N*-*N*-dimethylformanide and a surfactant stabilized aqueous SWNT suspension. The volume fraction of SWNTs in epoxy varied from 0.1 to 0.5%. The 0.5% volume fraction of SWNTs in epoxy enhanced the thermal conductivity by 27% over pure epoxy. The average interfacial resistance, R_{bd}, at the SWNT/matrix interface estimated by the effective medium theory was 4.27×10^{-8} m^2 K W^{-1} (the thermal boundary conductance, K_{bd} is 23.4 MW m^{-2} K^{-1}). Du *et al* [6] prepared isotropic SWNT/PMMA composites by a coagulation method [7] with different wt% of SWNTs. They concluded that there was no significant increase in thermal conductivity for the nanocomposites with loading up to 5 wt%. It increased, however, significantly at 7 wt% SWNT, most likely due to the SWNT/SWNT junctions, a primary cause for higher thermal conductivity relative to the polymer matrix. The experimental data reviewed above were used to validate our

Table 1. Parameters of polymers used for the simulation validation.

Polymers	Epoxy	PMMA[b]
Density, ρ (g cm^{-3})	1.20 ± 0.02[a]	1.19[b]
Thermal conductivity, λ (W m^{-1} K^{-1})	0.198[a]	0.21[b]
Specific heat, C (kJ kg^{-1} K^{-1})	1.22[c]	1.47[b]
Sound velocity, C_m (m s^{-1})	2400[d]	2400[d]

[a] Bryning *et al* [5].
[b] Technical data of Elson Plant (http://www.eslon-plant.jp).
[c] Technical data of Dow (http://www.dow.com).
[d] Bick *et al* [24].

computational model. Table 1 shows the technical data of epoxy and PMMA and the velocity of sound used for the model validation.

The presence of a resistance to the transfer of heat at the interface between the matrix material and the SWNT plays a very important role in the effective thermal conductivity. This thermal resistance is known as the Kapitza resistance [8]. According to the acoustic theory for the interpretation of thermal resistance [9], the probability for the transmission of phonons across the interface into the carbon nanotube, $f_{\text{m-CN}}$, is given by

$$f_{\text{m-CN}} = \frac{4}{\rho C C_m R_{bd}} \tag{1}$$

where ρ is the polymer density; C is the matrix specific heat; C_m is the sound velocity in the matrix and R_{bd} is the thermal boundary resistance. Even though nanotube–nanotube junctions could offer resistance to the transfer of heat between nanotubes as described in [6], the assumption used in this work is that a nanotube–matrix–nanotube transfer results in a higher thermal resistance than nanotube–nanotube transfer. A distinction between nanotube–polymer–nanotube and intimate nanotube–nanotube junctions is somewhat arbitrary, but it illustrates that phonons can be transferred from one nanotube to the next with or without the intermediate step of phonon transfer to the polymer. The Kapitza resistance at the matrix–SWNT interface is expected to play a dominant role in low wt% SWNT composites, and the nanotube–nanotube resistance is expected to play a significant role in high wt% SWNT composites. The preliminary molecular dynamics simulations of Maruyama *et al* [10] showed that the thermal boundary conductance between the SWNTs in a bundle is about 4 MW m^{-2} K^{-1}. This value is smaller than the values for the SWNT–epoxy and SWNT–PMMA composites, as found experimentally.

Tomadakis and Sotirchos [11] developed an algorithm to study the transport properties of random arrays of cylinders in a conductive matrix. However, the thermal resistance or the ratio of length to diameter of the dispersed phase was not taken into account. Duong *et al* [12] developed a new algorithm by taking into account the thermal resistance at the interfaces between carbon nanotube inclusions and matrix material. The developed algorithm was more effective than a typical random walk algorithm and much faster than a molecular dynamics algorithm [13, 14]. The carbon nanotube thermal conductivity was treated as effectively infinite, obviating the need to model random walks within the nanotubes. However, the model was only applied for the case of multi-walled carbon nanotubes, as the diameter of carbon nanotubes used in the simulations was much larger than the diameter of SWNTs determined by experiments. In addition, the value of the thermal equilibrium factor (see further discussion in section 2.3) was assumed to be one.

The present work modifies the previous model by taking into account the thermal equilibrium factor and using the real experimental parameters for SWNT properties. The thermal equilibrium factor for cylindrical SWNTs and the polymers is determined by a numerical method. The developed model is validated by experimental data for epoxy [5] and PMMA [6]. The different weight fraction of SWNTs in the polymers and the role of thermal interfacial resistance in the effective thermal conductivity of SWNT–polymer composites are also quantified in this work.

2. Simulation work

2.1. Parameters of the SWNT geometry used in the simulations

According to experimental measurements [15], the SWNT diameter is usually not greater than 3.0 nm, while the length of SWNTs dispersed in polymer can be up to several micrometers. Therefore, the aspect ratio of SWNTs, as found from experiments, is extremely large. Choosing a proper ratio of SWNT length, L, over the individual SWNT diameter, D, such that the SWNTs in the simulation runs represent well the experimental structure of the SWNT–polymer composite, is essential for the simulation runs, since it can reduce the computational domain size and the required simulation time.

Through the effective medium theory, the effective thermal conductivity of a composite material is a function of the geometry factor. Two composites with the same geometry factor, even if this corresponds to different inclusion shapes, are equivalent. The geometry factor is defined as a function of the ratio L/D as follows [16]:

$$G_f = \frac{p^2}{2\left(p^2-1\right)} - \frac{p}{2\left(p^2-1\right)^{3/2}} \cosh^{-1} p. \tag{2}$$

Here G_f is the geometry factor and $p = L/D$.

Figure 1 shows the geometry factor as a function of the aspect ratio L/D. As can be seen, when L/D is greater than 25, the geometry factor G_f is almost constant. This means that if the ratio L/D for the simulation runs is greater than 25, the effective thermal conductivity is no longer affected by the aspect ratio. To be conservative, the value $L/D = 40$ was used, and the SWNT diameter was set to be $D = 2.4$ nm.

2.2. Computational algorithm

The computation of the effective transport coefficients is based on an off-lattice Monte Carlo simulation of 90 000 walkers traveling in a computational cell for 100 ns. The computational domain for the numerical simulation is a cubic cell with SWNTs dispersed into the polymer matrix. It is divided in 96 bins on each side of the cube. The computational cell is

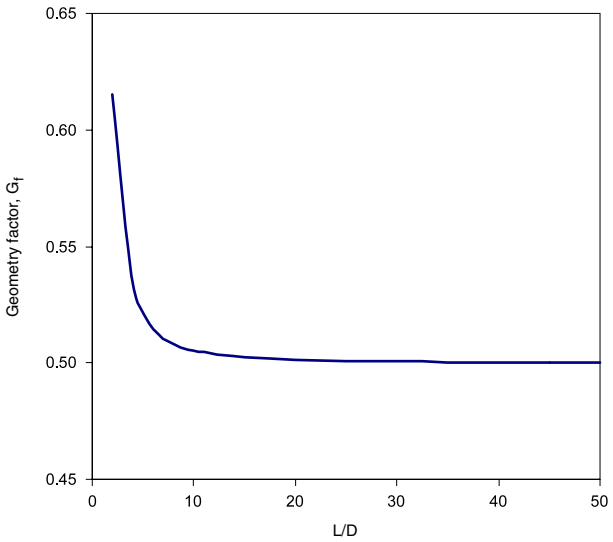

Figure 1. Effect of the aspect ratio L/D on the geometry factor.

heated from one surface (the $x = 0$ plane) with the release of 90 000 walkers distributed randomly and uniformly on that surface. The temperature distribution is calculated from the number of walkers found in each bin. The walkers exit at the surface opposite to the heated surface. The cell is periodic in the other two directions. The walkers move through the matrix material by Brownian motion [17]. The Brownian motion in each space direction is simulated with random jumps that each walker executes at each time step. These jumps take values from a normal distribution with a zero mean and a standard deviation

$$\sigma = \sqrt{2D_{\mathrm{m}}\Delta t} \tag{3}$$

where D_{m} is the thermal diffusivity of the matrix material and Δt is the time increment. Such a Brownian motion model has been used successfully to model heat transfer due to diffusion in the case of convective flows [18–20]. The adequacy of the number of walkers, and of the size of the computational domain, for the calculation of the effective thermal conductivity has been discussed in [12].

Once a walker in the matrix reaches the interface between the matrix and an SWNT, the walker will move into the SWNT phase with a probability $f_{\mathrm{m\text{-}CN}}$, which represents the thermal resistance of the interface, and will stay at the previous position in the matrix with a probability $(1 - f_{\mathrm{m\text{-}CN}})$. Similarly, once a walker is inside an SWNT, the walker will redistribute randomly within the SWNT with a probability $(1 - f_{\mathrm{CN\text{-}m}})$ at the end of a time step, and will cross into the matrix phase with a probability $f_{\mathrm{CN-m}}$.

In order to make the calculation of the effective thermal conductivity easy, we simulated heat transfer with constant heat flux through the computational domain, by releasing 'hot' walkers constantly from one side of the domain and by releasing an equal number of 'cold' walkers (carrying negative energy [21]) from the opposite side of the computational domain. The theoretical solution of this problem at steady state is a linear temperature profile whose slope is inversely proportional to the medium conductivity. This time-independent result was robust and trivial to fit, in contrast with the changing exponential profiles of a time-dependent problem.

The model assumptions are as follows.

(1) The walkers are distributed uniformly once inside the SWNTs due to the high SWNT thermal conductivity.
(2) The SWNTs are assumed to be dispersed in a way that they do not form bundles and do not bend, even though the algorithm is flexible enough to allow for the relaxation of this assumption. (One could allow the formation of bundles in the composite and, if the resistance to heat transfer between SWNTs were known, one could take it into account. One could also incorporate bending in the model by approximating a bent SWNT by a sequence of several rod-like SWNTs connected end-to-end.) However, the possible bundle effect is ignored in this work.
(3) The transfer of heat is passive.
(4) The thermal boundary resistance is the same for walkers coming in and out the SWNTs.
(5) The volume fraction of SWNTs in every slice (i.e., every x plane) of the computational domain is equal to the volume fraction of the SWNTs in the composite, so that the weighted average of the product of the density times the heat capacity for a slice of the composite is the same throughout the domain.
(6) The boundaries on the y and z sides are treated as periodic, while those on the x side (perpendicular to the applied flux) are treated as hard walls.

More details about the random walk algorithm can be found in Duong *et al* [12].

2.3. Determination of the thermal equilibrium factor of SWNTs and polymers

By making the assumption that the thermal walkers move randomly inside the SWNTs and that they are distributed with a uniform distribution instantaneously in the SWNTs, a length scale is removed from the physical problem. This length scale is the magnitude of the random Brownian jump that the thermal walkers should execute once inside the SWNTs. This assumption is very reasonable, when one takes into account that this length scale is very much larger than the size of the SWNT in our computational framework, because of the orders of magnitude difference in the thermal conductivity of the matrix and the SWNTs. In other words, during one time step in the computational model, the length scale that corresponds to the movement of a thermal walker in the matrix phase is of order σ, while the movement of a thermal walker in the SWNT is much larger within the same time step. Furthermore, in thermal equilibrium, the average walker density within the SWNTs should be equal to that in the matrix, ensuring that the second law of thermodynamics is not violated. Since the walkers can exit an SWNT from anywhere on the SWNT surface even one time step after they enter into it, we must weight the exit probability $f_{\mathrm{CN\text{-}m}}$ so that the flux of walkers into the SWNTs equals the flux of walkers going out when they are in equilibrium with the surrounding matrix. The

weight factor depends only upon geometry, since its goal is to achieve the correct walker density inside and outside the SWNT. To maintain equilibrium, the probability of a walker to enter an SWNT when it collides with its surface coming from the matrix, $f_{\text{m-CN}}$, and the probability of a walker to exit an SWNT when it collides with its surface coming from the SWNT interior, $f_{\text{CN-m}}$, are related as follows:

$$f_{\text{CN-m}} = C_{\text{f}} \frac{\sigma A_{\text{c}}}{V_{\text{c}}} f_{\text{m-CN}} \tag{4}$$

where A_{c} and V_{c} are the surface area and the volume of an SWNT respectively; σ is the standard deviation of the random jump in the matrix and C_{f} is a geometry-specific coefficient that can be called the *thermal equilibrium factor*. Equation (4), thus, reintroduces a length scale into the system by using the ratio $A_{\text{c}}/V_{\text{c}}$.

As already mentioned, the factor C_{f} guarantees that the second law of thermodynamics applies in our computational model. At thermal equilibrium there are two conditions that need to be satisfied: (a) the density of the thermal walkers inside the SWNTs and the density of the walkers in the matrix phase have to be equal, i.e., the temperature should be the same inside and outside the SWNTs, and (b) the heat flux into an SWNT has to be equal to the heat flux from the SWNT to the matrix phase, so that heat is not transferred from a cold area to a hot area. Equating the total number of thermal walkers entering a cylindrical nanotube with the number of walkers exiting the nanotube, and assuming that equation (4) holds, one can obtain the value for the thermal equilibrium factor $C_{\text{f}} = 1/(2\sqrt{\pi}) \cong 0.28$ for an infinite cylindrical inclusion in the matrix. This is done by taking into account that thermal walkers that enter an SWNT come from distances away from the SWNT surface that follow a normal distribution with zero mean and a standard deviation equal to σ, integrating, thus, the expression for the normal distribution probability density function from the SWNT surface to infinity. However, since the nanotubes in the present case are finite instead of infinite cylinders, C_{f} was determined by a numerical procedure as follows. The random walk algorithm described above was used to simulate thermal equilibrium for the case of only one SWNT having $D = 2.4$ nm and $L/D = 40$ within the polymer cell. The computation cell used was $96 \times 32 \times 32$ (cubic grid units) in the x, y and z directions, respectively. The SWNT having its axis parallel to the x direction was placed at the computational domain center and the thermal walkers were released uniformly in the domain and were allowed to reach equilibrium (instead of being released at $x = 0$). The number of walkers in this numerical experiment was 98 304 ($96 \times 32 \times 32$). Different values of C_{f}, ranging from 0.24 to 0.31 with a 0.01 interval, were used in the simulation runs. This range of values was chosen because our theoretical analysis for the thermal equilibrium factor C_{f} showed that the thermal equilibrium factor for an infinite cylindrical inclusion in the matrix is approximately 0.28. After a long simulation time, the walker distribution inside the domain was plotted at different positions of the computational cell. The value of the thermal equilibrium factor C_{f} is the one resulting in a uniform distribution of the walkers inside and outside of the SWNT.

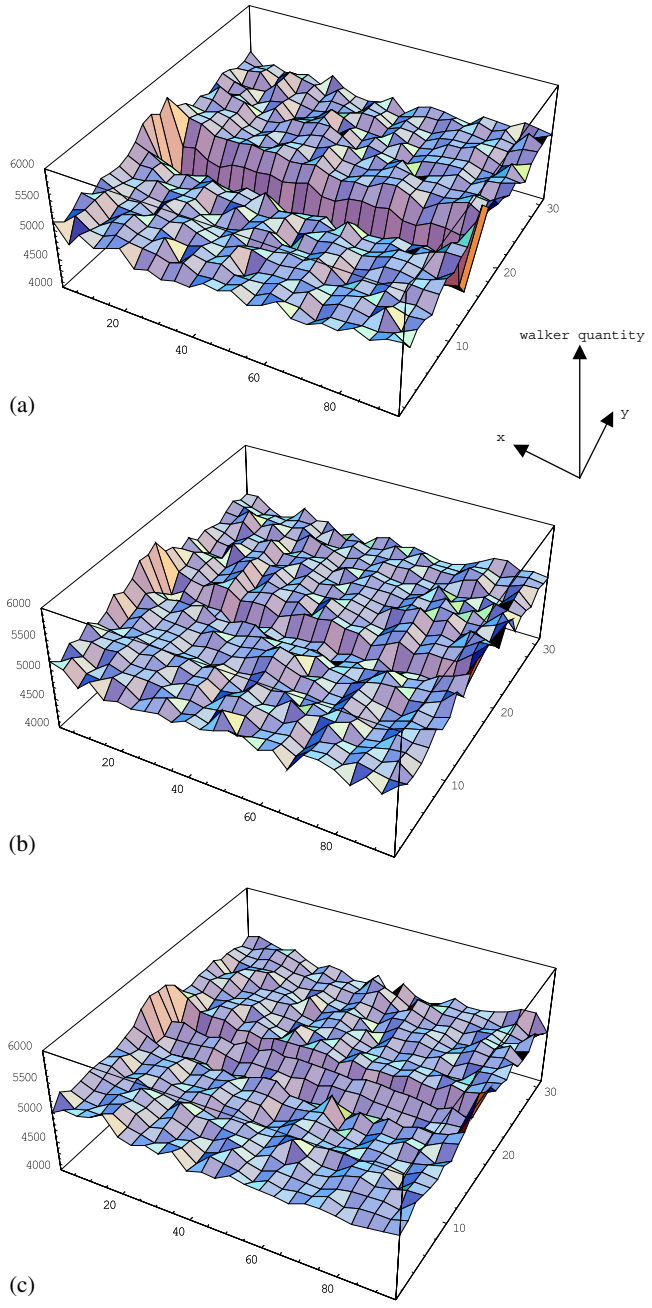

Figure 2. Walker distribution at the surface parallel to the x axis at the middle of the cell, at $z = 16$, with different thermal equilibrium factors: (a) $C_{\text{f}} = 0.28$; (b) $C_{\text{f}} = 0.25$; and (c) $C_{\text{f}} = 0.24$.

Our simulation results showed that the appropriate thermal equilibrium value was $C_{\text{f}} = 0.25$, and this value was used to obtain all simulation results shown from now on.

Figures 2(a)–(c) show that the walker distribution in the cell after equilibrium is obtained on a surface parallel to the x axis and cut at grid point $z = 16$, which is the middle of the cell. Figure 2(a) shows that more walkers cross the interface and remain in the polymer matrix, violating the second law of thermodynamics. Figure 2(c) shows that more walkers remain outside the SWNT. Figure 2(b) shows that the density of walkers inside and outside the SWNT is almost the same, establishing thermal equilibrium. The slight variation in

Table 2. Summary of the simulation parameters and simulation runs used for SWNT–PMMA composites.

Simulation parameters	Computational cell: $100 \times 100 \times 100$ nm^3 ($96 \times 96 \times 96$ grid^3) Number of walkers: 90 000 ($1 \times 300 \times 300$) Time increment: 0.0025 ns SWNT diameter: 2.4 nm Ratio L/D: 40 Thermal equilibrium value C_f: 0.25				
SWNT orientation in the cell	(1) SWNTs are perpendicular to the heat flux (2) SWNTs are parallel to the heat flux (3) SWNTs are randomly dispersed in polymers				
		Matrix probability, $f_{m\text{-}CN}$			
		0.02	0.20	0.50	1.00
		Thermal boundary resistance, R_{bd} (10^{-8} m^2 K W^{-1}) (Thermal boundary conductance, K_{bd} (MW m^{-2} K^{-1}))			
		SWNT–PMMA composites			
		5.50 (18.2)	0.55 (181.8)	0.22 (454.5)	0.11 (909.1)
		SWNT–epoxy composites[a]			
Weight fraction of SWNTs (wt%)	Number of SWNTs	5.69 (17.6)	0.57 (175.4)	0.23 (434.8)	0.11 (909.1)
0.10	55				
0.50	249				
1.00	454				
2.00	766	3 runs	3 runs	3 runs	3 runs
3.00	994				
5.00	1304				
7.00	1505				

[a] Simulation runs were done for the model validation with experimental data [5].

density at the surface is due to the choice of using a normal distribution for the steps of random walkers leaving the surface of the SWNT.

3. Results and discussion

3.1. Model validation with the experimental data of SWNT–epoxy and SWNT–PMMA composites

The computational model is validated with two different kinds of polymer, epoxy and PMMA. Table 2 summarizes the simulation parameters used, the simulation runs done for the PMMA–polymer composites with different $f_{m\text{-}CN}$, SWNT orientation and weight fraction of SWNTs in polymers. For each kind of SWNT orientation in the computational cell and each value of thermal boundary resistance and weight fraction of SWNTs, the thermal conductivity is the average of three simulations with different initial SWNT distributions.

The simulation results were compared with the experimental data of Bryning *et al* [5] for the SWNT–epoxy composites as shown in figure 3. The weight fraction error of the experimental data of Bryning *et al* [5] was reported to be ±10%. We

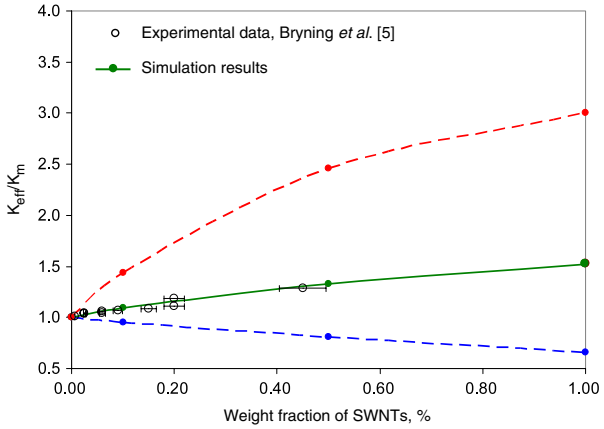

Figure 3. Validation of the computational model with comparison to experimental data for SWNT–epoxy composites. The upper and lower dashed curves indicate the potential maximum and minimum thermal conductivity, respectively. Dots on the dashed curves indicate the simulation results. The best fit line to the data (solid line) yields an $f_{m\text{-}CN}$ consistent with physical data.

ran the simulations with different values of the average probability for transmission of phonons across the interface into the SWNTs, $f_{m\text{-}CN}$. We found that the value of $f_{m\text{-}CN}$ giving the best fit between the simulation results and the experimental data for this experimental work is 0.02. Applying the acoustic theory, the thermal boundary resistance can then be calculated by equation (1) to be 4.01×10^{-8} m^2 K W^{-1}, very close to 4.27×10^{-8} m^2 K W^{-1}, the average thermal boundary resistance estimated by the effective medium theory [5, 16]. As can be seen in figure 3, the simulation results fit very well with the experimental data using this specific value of f_{m-CN}. The upper and the lower dashed curves indicate the maximum and minimum possible values of the thermal conductivity, respectively, as a function of the weight fraction of SWNTs dispersed in epoxy for the conditions reported in the experiments. Since the thermal boundary resistance between an SWNT and the epoxy has been obtained by the experimental data, this thermal boundary resistance of the SWNT–epoxy composites is then used for simulation runs with different weight fractions of the SWNTs and to determine the potential maximum and minimum of the SWNT–epoxy composites. The maximum thermal conductivity was obtained when all SWNTs were arranged with their axes parallel to the direction of the heat flux (the x direction) and the minimum thermal conductivity was obtained when all SWNTs were arranged with their axes perpendicular to the direction of the heat flux (the z direction).

Figure 4 shows simulation results compared to the experimental data of Du *et al* [6] for the SWNT–PMMA composites. The upper and the lower dashed curves indicate the potential maximum and minimum thermal conductivity, respectively, as a function of the weight fraction of SWNTs dispersed in PMMA for the experimental conditions of Du *et al* [6]. The thermal conductivity error of this work was reported to be ±15%. The thermal boundary resistance calculated by the computational model is 9.53×10^{-9} m^2 K W^{-1}. The thermal conductivity determined by experiments at 7% weight fraction of SWNTs in PMMA is higher than the simulation

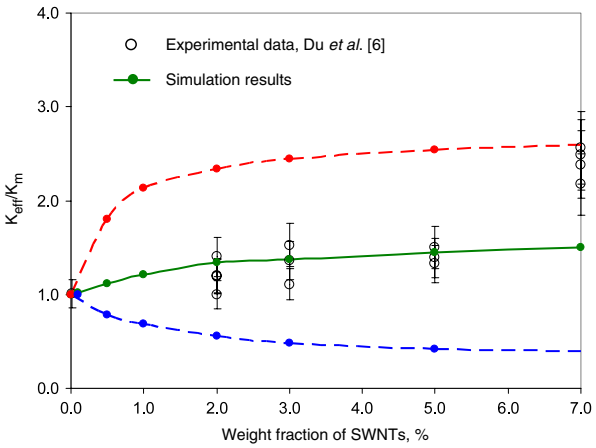

Figure 4. Validation of the computational model with comparison to experimental data of SWNT–PMMA composites. The upper and lower dashed curves indicate the potential maximum and minimum thermal conductivity, respectively. Dots on the dashed curves indicate the simulation results. The best fit line to the data (solid line) yields an $f_{\text{m-CN}}$ consistent with physical data.

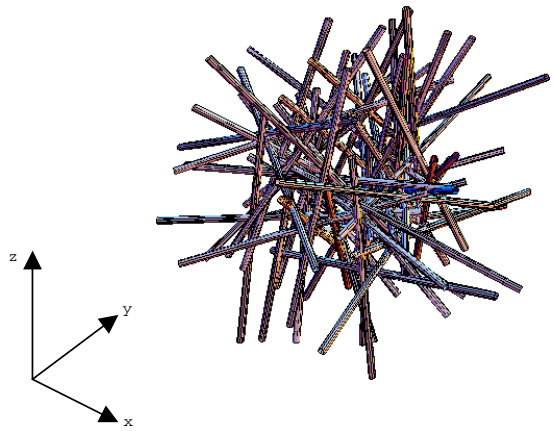

Figure 5. A model of SWNT composite material. The composite shown here is a realization of the case of disordered SWNTs at a weight fraction 0.10% and $L/D = 40.0$.

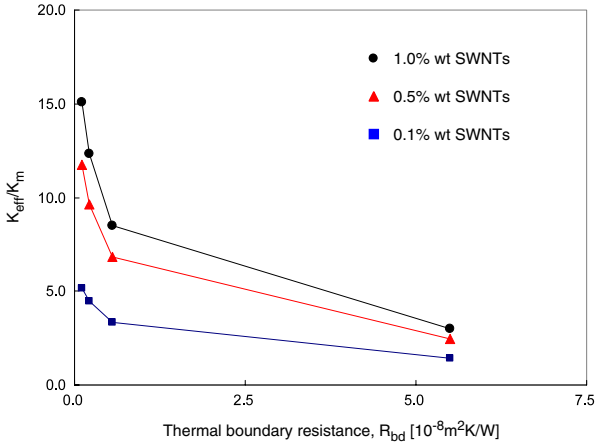

Figure 6. Effective thermal conductivity of SWNT–PMMA composites with SWNTs oriented parallel to the heat flux as a function of thermal boundary resistance with different weight fraction of SWNTs. For each value of thermal boundary resistance and weight fraction of SWNTs, the thermal conductivity is the average of three simulations with different initial SWNT distributions.

results. The reason for the discrepancy is that at high weight fraction (and, thus, high volume fraction) of SWNTs, the SWNT/SWNT junctions and agglomeration can cause heat to move more easily between SWNTs. The measured thermal conductivity for this case is higher than the simulation results, because our model did not take into account this factor. The difference in thermal boundary resistance in the SWNT–epoxy and SWNT–PMMA composites is perhaps the result of nanotube type, dispersion quality, nanotube purity and length, or the composite preparation procedure [5]. For example, raw SWNT material, not highly purified SWNTs, often contains significant carbonaceous and metallic impurities on the SWNT surface, which can adversely affect the composite performance and complicate the quantitative analysis of composite properties [5].

3.2. Effects of volume fraction of SWNTs and of thermal boundary resistance on the thermal conductivity of the SWNT–polymer composites

The heat flow was studied in a 100 nm size cubic cell containing 2.4 nm diameter SWNTs (these quantities are scaled). The SWNTs were perpendicular or parallel to the direction of heat flow or they were randomly oriented; in all cases the location of the SWNTs was random. The number of SWNTs in the cubic cell varied from 55 to 454 and depended on the weight fraction of SWNTs in the composite. The model of an SWNT composite material shown in figure 5 is a realization of the case of disordered SWNTs at a weight fraction 0.10% and $L/D = 40.0$. The simulations were conducted with three different orientations of SWNTs dispersed in the composites (parallel to the heat flux, perpendicular to the heat flux, and randomly oriented), with different thermal resistance ($f_{\text{m-CN}} = 1.00, 0.50, 0.20, 0.02$) and with different weight fraction of SWNTs (0.1%, 0.5% and 1.0%). The thermal conductivity was the average of three simulation runs with different initial SWNT random distributions. The matrix used for the simulations was PMMA. Figures 6–8 show the effective thermal conductivity of heat flux-parallel, randomly dispersed, and heat flux-perpendicular SWNT–PMMA composites, respectively, as a function of thermal boundary resistance with different weight fraction of SWNTs.

With the same thermal boundary resistance and weight fraction, the random jump of walkers in the heat flow direction is less (meaning worse heat transfer) for the SWNTs perpendicular to the heat flux, higher for the random distribution of the SWNTs, and maximum for the SWNTs parallel to the heat flux. This allows the heat walkers to diffuse more easily through the cell. Therefore, the thermal conductivity increases in these cases as expected. With the same thermal boundary resistance, the ratio of the maximum and the minimum thermal conductivity increases when increasing the weight fraction of SWNTs. With the

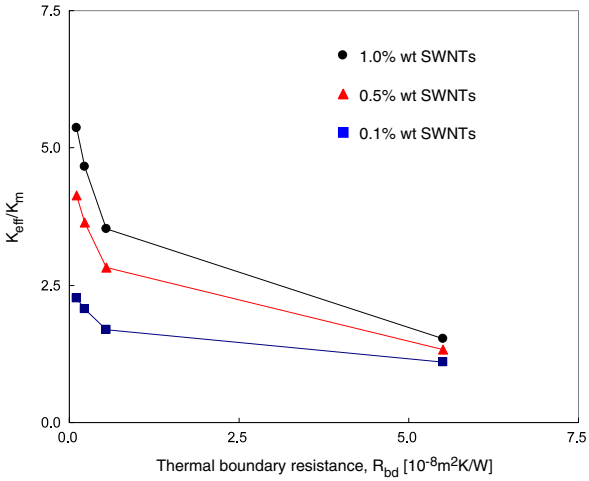

Figure 7. Effective thermal conductivity of randomly dispersed SWNT–PMMA composites as a function of thermal boundary resistance with different weight fraction of SWNTs. For each value of thermal boundary resistance and weight fraction of SWNTs, the thermal conductivity is the average of three simulations with different initial SWNT distributions.

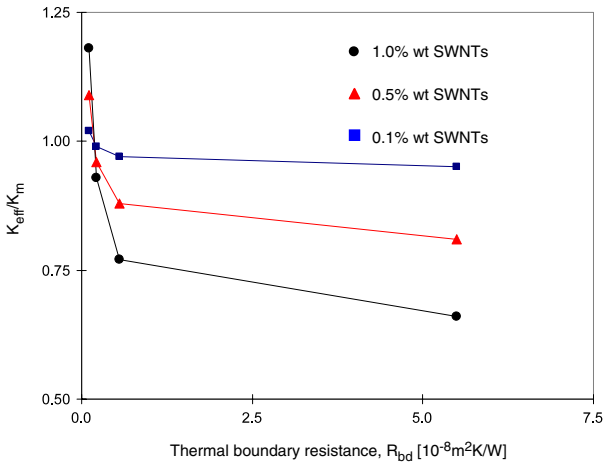

Figure 8. Effective thermal conductivity of SWNT–PMMA composites with SWNTs oriented perpendicular to the heat flux as a function of thermal boundary resistance with different weight fraction of SWNTs. For each value of thermal boundary resistance and weight fraction of SWNTs, the thermal conductivity is the average of three simulations with different initial SWNT distributions.

same weight fraction, this ratio decreases if the thermal boundary resistance increases. Duong *et al* [22] studied the thermophysical properties of SWNTs aligned vertically inside PMMA and concluded that the effective thermal conductivity of the SWNT–PMMA composite with approximately 0.1 wt% SWNTs could be enhanced significantly once the heat flow direction was parallel to the SWNT axes. So this work is complementary to the experimental work of Duong *et al* [22] in explaining the unusual thermal behavior of the SWNT–PMMA composite as measured by the photothermal radiometry technique.

Note that the effective thermal conductivity, K_{eff}, is still much lower than that calculated by the modified Maxwell theory for non-spherical inclusions, even in the case of heat transfer with SWNTs oriented parallel to the direction of heat transfer. The effective thermal conductivity can be calculated by the Maxwell theory modified by Rayleigh [23] as follows:

$$K_{\text{eff}} = (1 - \phi)\, K_{\text{m}} + \phi\, K_{\text{SWNT}} \tag{5}$$

where ϕ is the volume fraction of SWNTs; K_{m} and K_{SWNT} are the thermal conductivities of matrix and SWNTs, respectively. The thermal conductivity of 0.1% weight fraction (2.35% volume fraction) of SWNTs (thermal conductivity in the range 1750–6600 W m^{-1} K^{-1}) in epoxy can be calculated from equation (5) to be between 42.23 and 156.01 W m^{-1} K^{-1}, while the maximum thermal conductivity from the simulation is 1.02 W m^{-1} K^{-1} (calculated as five times higher than the pure epoxy value, according to figure 6). Note that the Maxwell equation does not take into account the effects of the thermal resistance at the matrix–inclusion interface, but it has been used in the past to make order of magnitude predictions for the performance of nanocomposites. The discrepancy observed in the present case demonstrates vividly the critical importance of the thermal resistance in the effective thermal conductivity.

Figure 8 shows that the thermal conductivity of SWNT–PMMA composites is smaller that of the pure PMMA when the SWNTs are perpendicular to the heat flow and the thermal boundary resistance is high. This is the result of a large number of SWNTs having very high thermal boundary resistance in the domain and forming a 'fire wall' that blocks the walkers from moving forward in the cell. This causes the thermal conductivity to be reduced dramatically.

4. Conclusions

A computational model for systematically studying the thermal conductivity of SWNT–polymer composites using a random walk algorithm has been successfully developed. The simulation consumes much less time than molecular dynamics simulations. The simulation results agree well with experimental data for SWNT–PMMA and SWNT–epoxy composites. A key to the application of the numerical method is the determination of the thermal equilibrium factor of SWNTs and polymers. A computational method to determine this factor is presented.

This model can be applied to any polymer and any solid materials with a very wide range of volume fraction of SWNTs in the matrix, given that the inclusions are not in contact with each other. The maximum and minimum possible thermal conductivity can thus be determined, according to the orientation of the SWNTs in the composite. The model works well with a small weight fraction of SWNTs dispersed in polymers (up to 5 wt% of SWNTs). When fewer SWNTs are dispersed in the polymers, more inclusions are not in contact with each other. This assumption appears to break down with higher than 5 wt% of SWNTs in the epoxy due to considerable contact between SWNTs (see figure 4). However, the computational model is flexible enough to be able to incorporate nanotube–nanotube resistance, if one could obtain

information about the value of the thermal resistance at the nanotube–nanotube junction.

Acknowledgments

This work was supported in part through the 21st Century COE Program, 'Mechanical Systems Innovation', by the Ministry of Education, Culture, Sports, Science and Technology, Japan, by the National Computational Science Alliance under CTS-040023 and by the TeraGrid under TG-CTS070037T, USA; it utilized the NCSA IBMp690, USA.

References

[1] Ajayan P M, Schadler L S, Giannaris C and Rubio A 2000 *Adv. Mater.* **12** 750
[2] Choi S U S, Zhang Z G, Yu W, Lockwood F E and Grulke E A 2001 *Appl. Phys. Lett.* **79** 2252
[3] Biercuk M J, Llaguno M C, Radosavljevic M, Hyun J K, Johnson A T and Fischer J E 2002 *Appl. Phys. Lett.* **80** 2767
[4] Wagner H D, Lourie O, Feldman Y and Tenne R 1998 *Appl. Phys. Lett.* **72** 188
[5] Bryning M B, Milkie D E, Kikkawa J M and Yodh A G 2005 *Appl. Phys. Lett.* **87** 161909
[6] Du F, Guthy C, Kashiwagi T, Fischer J E and Winey K I 2006 *J. Polym. Sci.* B **44** 1513
[7] Du F, Fischer J E and Winey K I 2003 *J. Polym. Sci.* B **41** 3333
[8] Kapitza P L 1941 *J. Phys. USSR* **4** 181
[9] Swartz E T and Pohl R O 1989 *Rev. Mod. Phys.* **61** 605
[10] Maruyama S, Igarashi Y, Taniguchi Y and Shiomi J 2006 *J. Therm. Sci. Tech.* **1** 138
[11] Tomadakis M M and Sotirchos S V 1992 *J. Chem. Phys.* **104** 6893
[12] Duong M H, Papavassiliou D V, Mullen J K and Lloyd L L 2005 *Appl. Phys. Lett.* **87** 013101
[13] Maruyama S and Kimura T 1999 *Therm. Sci. Eng.* **7** 63
[14] Huxtable S *et al* 2003 *Nat. Mater.* **2** 731
[15] Murakami Y, Einarsson E, Edamura T and Maruyama S 2005 *Carbon* **43** 2664
[16] Nan C W, Shi Z and Lin Y 2003 *Chem. Phys. Lett.* **375** 666
[17] Einstein A 1905 *Ann. Phys., Lpz.* **17** 549
[18] Papavassiliou D V and Hanratty T J 1997 *Int. J. Heat Mass Transfer* **40** 1303
[19] Mitrovic B M, Le P M and Papavassiliou D V 2004 *Chem. Eng. Sci.* **59** 543
[20] Le P M and Papavassiliou D V 2006 *J. Heat Transf. Trans. ASME* **128** 53
[21] Sundqvist B, Sandberg O and Backstrom G 1977 *J. Phys. D: Appl. Phys.* **10** 1397
[22] Duong H M, Mori Y, Einarsson E, Nagasaka Y and Maruyama S 2007 *Proc. 8th Asian Thermophysical Properties Conf. (Fukuoka, Japan)* p 160
[23] Bird R B, Stewart W S and Lightfoot E N 2002 *Transport Phenomena* 2nd edn (New York: Wiley) p 282, 376 and 379
[24] Bick A and Dorfmueller T 1989 Light scattering study of epoxy resin polymerization reactive and flexible molecules in liquids *NATO ASI Series C* vol 2910, p 389